FEBS Open Bio 4 (2014) 60–64

ELSEVIER

CrossMark

FEBS openbio

journal homepage: www.elsevier.com/locate/febsopenbio

1964–2014

Trim27-deficient mice are susceptible to streptozotocin-induced diabetes☆

Mohammad Mahabub-Uz Zaman, Toshie Shinagawa, Shunsuke Ishii*

Laboratory of Molecular Genetics, RIKEN Tsukuba Institute, 3-1-1 Koyadai, Tsukuba, Ibaraki 305-0074, Japan
University of Tsukuba, Graduate School of Comprehensive Human Sciences, Tsukuba, Ibaraki 305-8577, Japan

ARTICLE INFO

Article history:
Received 7 November 2013
Received in revised form 29 November 2013
Accepted 16 December 2013

Keywords:
TRIM27
Disease
Diabetes
TNF-α
Apoptosis

ABSTRACT

Tumor necrosis factor α (TNF-α) plays an important role in cell proliferation and apoptosis, and defects in TNF-α-induced apoptosis are associated with various diseases. TRIM27 is a tripartite motif (TRIM) protein containing RING finger, B-box, and coiled-coil domains. We recently reported that TRIM27 positively regulates TNF-α-induced apoptosis through deubiquitination of receptor-interacting protein 1 (RIP1). Multiple studies have suggested a link between TNF-α pathway and various diseases, such as diabetes and colitis. Here, we report that *Trim27*-deficient mice were susceptible to streptozotocin (STZ)-induced diabetes, a mouse model of diabetes. Infiltration of T cells and cleaved caspase-3 signals were enhanced, and β-cell mass was decreased in *Trim27*-deficient islets compared to wild-type islets. On the other hand, *Trim27*-mutation did not affect the dextran sodium sulphate (DSS)-induced colitis. These data support the idea that the *TRIM27* mutation is responsible for the development of certain types of diseases.

1. Introduction

TRIM27 (also known as the Ret finger protein, RFP) is a member of the tripartite motif (TRIM) family of proteins containing the RBCC motif, which consists of the RING (really interesting new gene 1) finger, one or two B-box motifs, and a coiled-coil region [1]. TRIM27 was originally found to be fused to the *ret* proto-oncogene in transformed NIH3T3 cells [2]. The RING finger plays an important role in ubiquitin (Ub) E3 ligase binding to Ub-conjugating enzymes (E2) [3]. TRIM27 shuttles between the cytoplasm and the nucleus [4], and we recently demonstrated that cytosolic TRIM27 positively regulates tumor necrosis factor-α (TNF-α)-induced apoptosis [5]. TRIM27 forms a complex with and ubiquitinates the ubiquitin-specific protease USP7, which results in USP7 activation. Subsequently, USP7 deubiquitinates the receptor-interacting protein 1 (RIP1), resulting in positive regulation of TNF-α-induced apoptosis.

Dysregulation of TNF superfamily signaling is often correlated with various diseases, including diabetes and colitis [6]. For instance, mutant mice lacking TRAIL (TNF-related apoptosis-inducing ligand) are prone to STZ-induced diabetes [7]. This susceptibility is caused by a defect in the negative selection of thymocytes and the generation of autoreactive T cells. Furthermore, TNF-α signaling in macrophages and neutrophils is required for leukocyte infiltration of the DSS-treated colon, resulting in mucosal damage [8]. However, no empirical evidence indicating a linkage between TRIM27 and disease was reported. Here, we report that *Trim27*-deficient mice are susceptible to STZ-induced diabetes, a mouse model of diabetes.

2. Materials and methods

2.1. Mice

Trim27$^{-/-}$ C57BL/6 congenic mice generated by homologous recombination were described previously [5]. All mice used for experiments were 8–10 weeks old. Experiments were conducted in accordance with the guidelines of the Animal Care and Use Committee of the RIKEN Institute.

2.2. STZ-induced diabetes

For the STZ-induced diabetes model, male mice aged 8 weeks were injected intraperitoneally for 5 consecutive days with STZ (Sigma) dissolved in citrate buffer (pH 4.5), at a concentration of 40 mg/kg (multiple low doses), as described previously [9]. Blood glucose levels were measured weekly in blood collected from the tail vein of non-fasted animals during the noon time (between 2 to 3 pm), using a glucometer (Sanwa Kagaku Kenkyusho Co., Ltd., Japan). For

Abbreviations: DSS, dextran sodium sulphate; H&E, hematoxylin and eosin; RIP1, receptor-interacting protein 1; STZ, streptozotocin; TNF-α, tumor necrosis factor-α; TRIM, tripartite motif; Ub, ubiquitin.

* Corresponding author at: Laboratory of Molecular Genetics, RIKEN Tsukuba Institute, 3-1-1 Koyadai, Tsukuba, Ibaraki 305-0074, Japan. Tel.: +81 29 836 9031; fax: +81 29 836 9030.

E-mail address: sishii@rtc.riken.jp (S. Ishii).

2211-5463/$36.00
http://dx.doi.org/10.1016/j.fob.2013.12.002

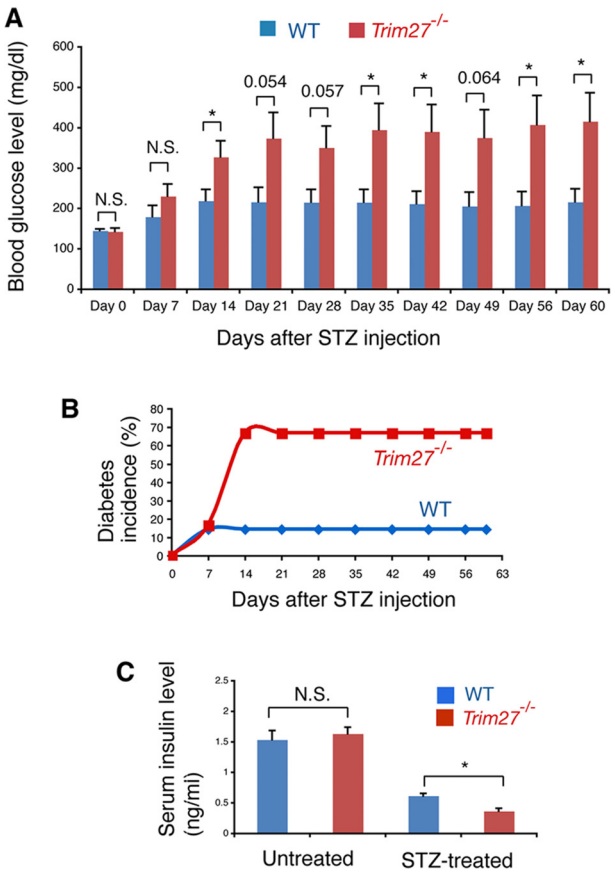

Fig. 1. *Trim27*$^{-/-}$ mice are prone to STZ-induced diabetes. (A and B) Blood glucose levels in WT and *Trim27*$^{-/-}$ mice after STZ injection. Mice were injected intraperitoneally with STZ, and blood glucose levels were measured weekly. Mean values ± SEM (WT, $n = 6$; *Trim27*$^{-/-}$, $n = 7$) are shown (A). Animals were considered diabetic when the blood glucose level exceeded 300 mg/dL (B). (C) Serum insulin levels in control (no treatment), and STZ-treated mice at 60 days after the first STZ injection. Each bar represents the mean ± SEM (WT, $n = 6$; *Trim27*$^{-/-}$, $n = 7$). * $p < 0.05$; N.S., no significant difference.

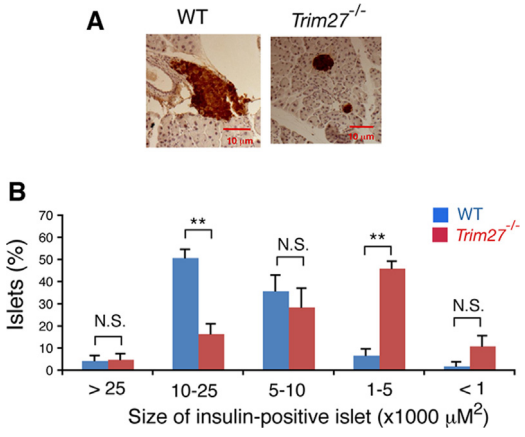

Fig. 2. Decreased β-cell mass in STZ-treated *Trim27*$^{-/-}$ mice. (A) Mice were injected intraperitoneally with STZ. At 60 days after the first STZ injection, pancreatic sections were immunostained with anti-insulin antibody, and representative sections are shown. (B) The size and frequency of insulin-positive islets were measured. Islet size was averaged from six WT and seven *Trim27*$^{-/-}$ mice, using three sections from each animal. The average frequency ± SEM of insulin-positive islets is shown as a bar graph. ** $p < 0.01$; N.S., no significant difference.

serum insulin measurements, non-fasting blood was collected from the saphenous vein, before sacrifice. The serum samples were snap frozen in liquid nitrogen, and stored at −80 °C until analysis of insulin concentration with a mouse ELISA kit (Mercodia).

2.3. DSS (dextran sodium sulphate)-induced colitis

Acute and chronic colitis were induced in 8- to 10-week-old mice by addition of DSS [MP Biomedicals, MW: 36,000–50,000 Da] in their drinking water, as described previously [10–12]. For acute colitis induction, mice were given 2% DSS in their drinking water for 7 days. For chronic colitis induction, mice were given 2% DSS in their drinking water for 1 week, followed by 1 week of regular water. This cycle was repeated three times, and mice were sacrificed at the end of the third cycle. Colitis was measured by daily monitoring of weight loss, and diarrhea development in each mouse.

2.4. Histological analysis

In the STZ-induced diabetes model, mice were sacrificed 60 days after the first STZ injection, and the whole pancreas was collected, fixed in 4% paraformaldehyde and embedded in paraffin. Sections were prepared from three parts of the pancreas, and stained with hematoxylin and eosin (H&E) to determine the degree of lymphocyte infiltration.

In the DSS-induced colitis model, mice were sacrificed after the end of the DSS treatment, and the abdominal cavity was exposed by midline laparotomy, and the entire colon was removed. The length of the colon was measured, and the colon was flashed with cold PBS, cut into several pieces, fixed in 4% formaldehyde and paraffin embedded. Several colon sections (5 μm) were prepared from the paraffin block, and stained with H&E for histological assessment of colitis.

2.5. Immunohistochemistry

In the STZ-induced diabetes model, pancreatic sections were analyzed by immunohistochemistry using anti-insulin (C27C9, Cell Signaling Technology), anti-CD3 (Abcam), and anti-cleaved caspase-3 (Cell Signaling Technology) antibodies, as described previously [9]. In brief, sections were deparaffinized and dehydrated in graded series of ethanol washes. Tissue sections were subjected to heat-induced epitope retrieval (10 mM citrate buffer boiled in a 500 watt microwave for 15 min), and then cooled at room temperature for 20 min. After washing in PBS, endogenous peroxidase was quenched using a 3% solution (v/v) of hydrogen peroxide in methanol. After blocking with PBS/3% BSA, sections were incubated with the primary antibodies overnight at 4 °C. Sections were then incubated with the secondary antibody, washed again in PBS, incubated for 10 min with DAB solution, and counterstained with hematoxylin. The insulin, cleaved caspase-3, and CD3 antibodies were used at a concentration of 1/1000, 1/800, and 1/100, respectively.

3. Results

3.1. Trim27$^{-/-}$ mice are prone to STZ-induced diabetes

It was reported that mutant mice lacking TRAIL (TNF-related apoptosis-inducing ligand) are prone to STZ-induced diabetes [16]. We therefore examined the susceptibility of *Trim27*$^{-/-}$ mice to STZ-induced diabetes, an animal model of diabetes, which is thought to arise after an autoimmune attack on pancreatic islets involving T cells and macrophages [13]. Multiple low doses of STZ were injected into wild-type (WT) and *Trim27*$^{-/-}$ mice. Starting from experimental day 14, all *Trim27*$^{-/-}$ mice showed progressively elevated serum glucose levels. Assessment of blood glucose levels in *Trim27*$^{-/-}$ and WT mice showed that *Trim27*$^{-/-}$ mice had significantly higher blood glucose levels than WT mice at 14, 35, 42, 56, and 60 days after the first STZ injection (Fig. 1A). By contrast, none of the WT mice developed diabetes. *Trim27*$^{-/-}$ mice showed a significantly higher incidence of

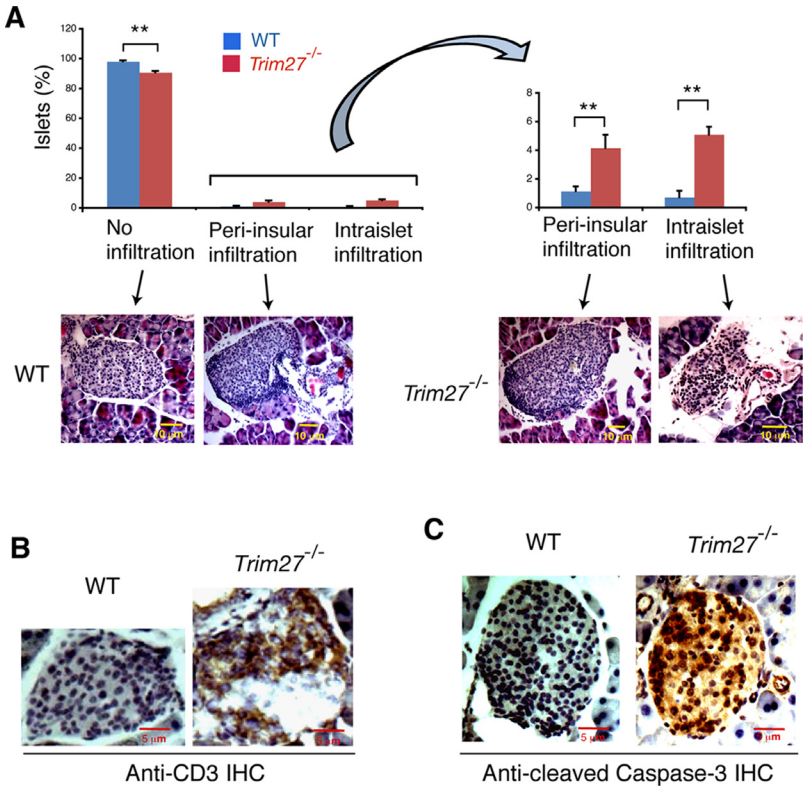

Fig. 3. Enhanced T-cell infiltration and cleaved caspase-3 in STZ-treated *Trim27*$^{-/-}$ islets. (A) Mice were injected intraperitoneally with STZ. At 60 days after the first STZ injection, pancreatic sections were stained with hematoxylin and eosin. An average of 75 sections (5 μm thickness) from each WT ($n = 6$) and *Trim27*$^{-/-}$ ($n = 7$) mouse were examined. The degree of infiltration was classified into three types, and the frequency was calculated. The average frequency ± SEM is shown as a bar graph (upper), and typical sections are shown (below). (B and C) Mice were injected intraperitoneally with STZ. At 60 days after the first STZ injection, pancreatic sections were immunostained with anti-CD3 (A) or anti-cleaved caspase-3 (C) antibodies, and typical sections are shown.

diabetes than WT mice, and all *Trim27*$^{-/-}$ mice became diabetic by experimental day 14 (Fig. 1B). Consistent with these results, significant hypoinsulinemia was detected in *Trim27*$^{-/-}$ mice at day 60 after the first STZ injection, which was greater than in WT mice (Fig. 1C).

3.2. Decreased β-cell mass in STZ-treated *Trim27*$^{-/-}$ mice

Together with an enhanced deterioration in glucose homeostasis after STZ treatment, *Trim27*$^{-/-}$ mice showed a reduction of the insulin-positive areas per islet (Fig. 2A). We quantified the islet number and size at 60 days after the first STZ injection, using the sections prepared from six WT and seven *Trim27*$^{-/-}$ mice. The number of large islets (10,000–25,000 μM^2) in *Trim27*$^{-/-}$ mice was lower than that in WT mice (Fig. 2B). On the other hand, the number of small islets (1000–5000 μM^2) in *Trim27*$^{-/-}$ mice was higher than that in WT mice. Thus, the decrease in islet number in *Trim27*$^{-/-}$ mice was evident at 60 days after the first STZ injection.

3.3. T-cell infiltration and cleaved caspase-3 are enhanced in STZ-treated *Trim27*$^{-/-}$ islets

To investigate whether the increased sensitivity of *Trim27*$^{-/-}$ mice to the diabetogenic effects of STZ was associated with exaggerated insulitis, pancreatic sections were histologically examined. The degree of infiltration was classified into three types, based on the description by Flodström et al. [13]: no infiltration, peri-insular infiltration, and intraislet infiltration. The number of islets without infiltration in *Trim27*$^{-/-}$ mice was significantly lower than in WT mice (Fig. 3A). On the other hand, the number of islets with peri-insular infiltration, and intraislet infiltration was significantly increased in *Trim27*$^{-/-}$ mice compared to WT mice (Fig. 3A).

To examine the type of infiltrating cells we immunostained the islet sections with anti-CD3 antibody, a general marker for T lymphocytes, and found that many of the *Trim27*$^{-/-}$ islets were infiltrated by CD3-positive T cells (Fig. 3B). Previous studies have shown that β-cell apoptosis is responsible for the development of insulin-dependent diabetes mellitus in the multiple low dose STZ model [14], and that cytokines secreted by infiltrating T lymphocytes, such as IL-1β and IFN-γ, play an important role in β-cell apoptosis [15–17]. Therefore, we examined the apoptosis-inducing enzyme, cleaved caspase-3 in *Trim27*$^{-/-}$ islets. Many of the islets were positive for cleaved caspase-3, indicating that apoptosis was induced (Fig. 3C).

3.4. *Trim27*$^{-/-}$ mice are not susceptible to DSS-induced colitis

Previous studies showed that TNF-α signaling in macrophages and neutrophils is required for leukocyte infiltration of the DSS-treated colon, resulting in mucosal damage [8], which is an animal model of ulcerative colitis. We therefore examined the susceptibility of *Trim27*$^{-/-}$ mice to DSS-induced colitis, which is characterized by epithelial disruption resulting in luminal bacterial translocation, and subsequent infiltration of immune cells [18]. There are two types of experimental models, acute and chronic DSS-induced colitis models, in which mice are treated with 2% DSS in the drinking water [10,11]. There was no abnormality in the histology of colon of WT and *Trim27*$^{-/-}$ mice (Fig. 4A). In the acute DSS-induced colitis model, the body weight of WT and *Trim27*$^{-/-}$ mice decreased at a similar rate after 2% DSS administration (Fig. 4B). Seven days after DSS administration, the mean body weight was reduced by 24% in WT, and 25% in *Trim27*$^{-/-}$ mice, and the observed difference was not significant (Fig. 4B). Moreover, there was no significant difference in colon

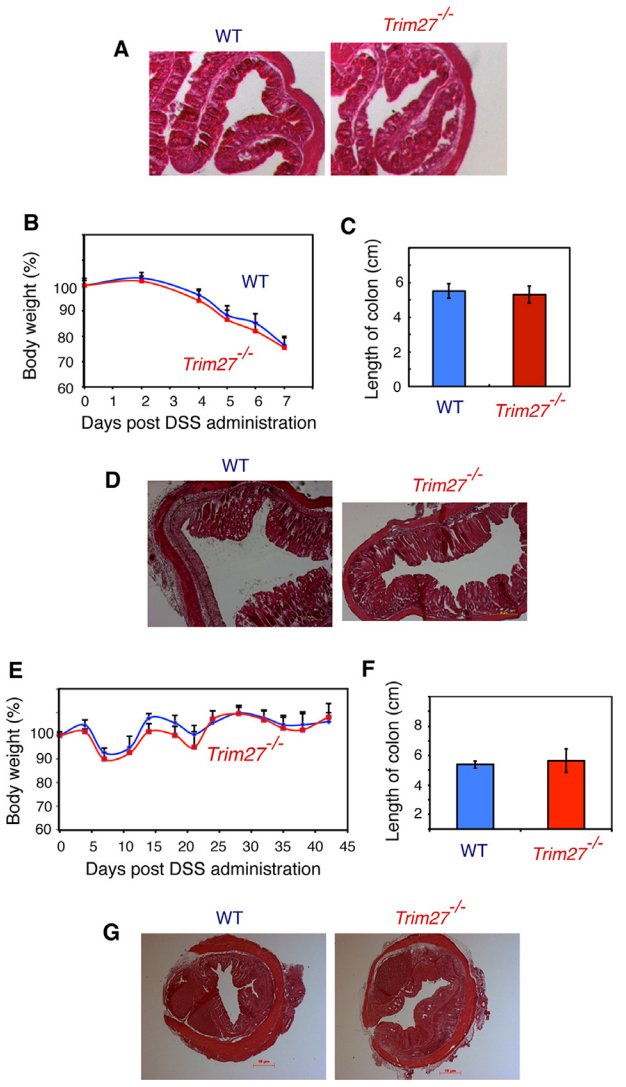

Fig. 4. *Trim27*-deficient mice are not susceptible to DSS-induced colitis. (A) No histological abnormality in the colon of WT and *Trim27*$^{-/-}$ mice. (B–G) Susceptibility of WT and *Trim27*$^{-/-}$ mice to acute (B–D) and chronic (E–G) DSS-induced colitis, using 2% DSS was examined. The body weight of WT and *Trim27*$^{-/-}$ mice was measured at the indicated times after DSS administration (B and E). Mean value ± SEM (acute colitis: male WT, $n = 4$; *Trim27*$^{-/-}$, $n = 6$; chronic colitis: female $n = 5$ for each WT and *Trim27*$^{-/-}$) is shown. The length of the colon was measured 7 (C) or 42 (F) days after DSS administration, and the mean value is shown with SEM (acute colitis: WT, $n = 4$; *Trim27*$^{-/-}$, $n = 6$; chronic colitis: $n = 5$ for each WT and *Trim27*$^{-/-}$) (D and G) Formalin-fixed colon sections were stained with H&E, 7 (D) or 42 (G) days after DSS administration.

length between WT and *Trim27*$^{-/-}$ mice 7 days after DSS administration (Fig. 4C). Colons from WT and *Trim27*$^{-/-}$ mice were analyzed by sectioning and H&E staining 7 days after DSS administration, and the results revealed histological alterations, such as loss of the entire crypt and desquamation of the surface epithelium, in both WT and *Trim27*$^{-/-}$ colons (Fig. 4D). In the chronic DSS-induced colitis model, there was no significant difference in the reduction of body weight (Fig. 4E), the reduction in colon length (Fig. 4F), and histological alterations in colons (Fig. 4G) between WT and *Trim27*$^{-/-}$ colons. Thus, *Trim27*-deficient mice are not susceptible to DSS-induced colitis.

4. Discussion

The results of the present study indicate that a loss of TRIM27 enhances STZ-induced diabetes, an animal model of diabetes. Recently, we reported that *Trim27*$^{-/-}$ mice are resistant to TNF-α induced apoptosis [5]. Consistent with the well-known concept that defects in apoptosis are frequently associated with multiple diseases, we found that *Trim27*$^{-/-}$ mice were susceptible to STZ-induced diabetes. This is consistent with the recent report, in which a linkage between *TRIM27* mutations and type 1 diabetes was suggested by more than 30 genome-wide association studies [19]. Since there was no difference in the levels of blood glucose and insulin and also in the colon abnormality between non-drug-treated WT and *Trim27*$^{-/-}$ mice, it is unlikely that TRIM27 would have a role in the development of different kind of diseases which secondary affect the incidence of STZ-induced diabetes.

Lymphocyte apoptosis plays a major role in immune tolerance, which is maintained through deletion of self-reactive lymphocytes (by cell death), functional inactivation (anergy), or suppression of cell activation via regulatory lymphocytes [20]. Members of the TNF and TNFR family play key roles in the development and function of the immune system. Defects in the TNFR family receptors or their downstream signaling pathways have been linked to uncontrolled lymphocyte proliferation in peripheral lymphoid organs, and the development of autoimmune diseases in mice and humans [20–22]. Mutant mice lacking TRAIL (TNF-related apoptosis-inducing ligand) are prone to STZ-induced diabetes [7]. This susceptibility is caused by a defect in the negative selection of thymocytes and the generation of autoreactive T cells. In addition, TRAF6 deficiency induces autoimmunity by affecting the development of thymic stroma cells [23]. Molecular and genetic analyses of Fas and FasL indicate that mouse lymphoproliferation and generalized lymphoproliferative disease are caused by mutations of Fas and FasL, respectively. These mutant mice develop lymphadenopathy by accumulating abnormal T cells, and suffer from systemic lupus erythematosus-like autoimmune disease [24]. Moreover, genetic deficiencies of IL-2 or its receptor, which are crucial elements for T-cell susceptibility to antigen-induced apoptosis, lead to lymphoid hyperplasia and autoimmunity [20].

Although in this study we couldn't show any direct evidence in support of the mechanism of crosstalk between defective apoptosis and development of diabetes. However, as the *Trim27*$^{-/-}$ mice showed increased infiltration of lymphocyte in the pancreas in response to STZ, we speculate that peripheral lymphocyte homeostasis and self tolerance mechanism to minimize the accumulation of autoreactive lymphocytes might be defective in *Trim27*$^{-/-}$ mice due to abrogated TNF-α-induced apoptosis. Increased autoreactive lymphocytes may attack the islet, which causes a decrease in islet mass. A recent study that used *Trim27*-deficient mice, which were independently generated from ours, showed that CD4 T cells of *Trim27*$^{-/-}$ mice can produce increase amount of cytokines under activated condition [25]. This could be another causative reason of increased sensitivity of *Trim27*$^{-/-}$ beta cells to STZ. As TRIM27 is widely expressed in many types of immune cells, including thymocytes, thymic stroma cells, and peripheral T cells, further analysis will be required to elucidate the mechanism by which the loss of TRIM27 affects the development of diabetes.

There was no difference in the susceptibility to acute and chronic DSS-induced colitis between WT and *Trim27*$^{-/-}$ mice. Multiple mechanisms by which TNF-α signaling regulates colitis were reported. TNF-α signaling in macrophages and neutrophils is required for leukocyte infiltration of the DSS-treated colon, resulting in mucosal damage [8]. Therefore, a defect in TNF-α-induced apoptosis in *Trim27*$^{-/-}$ leukocytes could enhance DSS-induced colitis. NF-κB activation by TNF-α is required for maintenance of intestinal epithelial cells, and intestinal epithelial cell-specific inhibition of NF-κB leads to apoptosis of colonic epithelial cells [26]. Hence, a defect in TNF-α-induced apoptosis in

Trim27$^{-/-}$ epithelial cells may prevent DSS-induced colitis. Finally, a defect in the TNF-α-induced apoptosis of intestinal epithelial cells through loss of caspase-8, leads to the development of inflammatory lesions via enhanced necroptosis of Paneth cells [27]. However, it is still unknown whether a defect in TNF-α-induced apoptosis through loss of TRIM 27 has a similar effect. Although an opposite role of TNF-α-induced apoptosis in leukocytes and epithelial cells, might explain why *Trim27*$^{-/-}$ mice are not susceptible to DSS-induced colitis, further studies are needed to clarify this issue.

In summary, we found that *Trim27*-deficient mice were susceptible to streptozotocin (STZ)-induced diabetes, a mouse model of diabetes. This finding may be useful to understand the mechanism of human diabetes.

Acknowledgements

We are grateful to the members of the Experimental Animal Division of the RIKEN Tsukuba Institute for maintenance of the mice. This work was supported in part by Grants-in-Aid for Scientific Research from the Ministry of Education, Culture, Sports, Science and Technology of Japan.

References

[1] Meroni, G. and Diez-Roux, G. (2005) TRIM/RBCC, a novel class of 'single protein RING finger' E3 ubiquitin ligases. Bioessays 27, 1147–1157.
[2] Takahashi, M., Ritz, J. and Cooper, G.M. (1985) Activation of a novel human transforming gene, ret, by DNA rearrangement. Cell 42, 581–588.
[3] Joazeiro, C.A. and Weissman, A.M. (2000) RING finger proteins: mediators of ubiquitin ligase activity. Cell 102, 549–552.
[4] Harbers, M., Nomura, T., Ohno, S. and Ishii, S. (2001) Intracellular localization of the Ret finger protein depends on a functional nuclear export signal and protein kinase C activation. J. Biol. Chem. 276, 48596–48607.
[5] Zaman, M.M., Nomura, T., Takagi, T., Okamura, T., Jin, W. and Shinagawa, T., et al. (2013) Ubiquitination-deubiquitination by the TRIM27-USP7 complex regulates TNF-α-induced apoptosis. Mol. Cell. Biol. 33, 4971–4984 http://dx.doi.org/10.1128/MCB.00465--13.
[6] Croft, M. (2009) The role of TNF superfamily members in T-cell function and diseases. Nat. Rev. Immunol. 9, 271–285.
[7] Lamhamedi-Cherradi, S.E., Zheng, S.J., Maguschak, K.A., Peschon, J. and Chen, Y.H. (2003) Defective thymocyte apoptosis and accelerated autoimmune diseases in *TRAIL*$^{-/-}$ mice. Nat. Immunol. 4, 255–260.
[8] Popivanova, B.K., Kitamura, K., Wu, Y., Kondo, T., Kagaya, T. and Kaneko, S. (2008) Blocking TNF-α in mice reduces colorectal carcinogenesis associated with chronic colitis. J. Clin. Invest. 118, 560–570.
[9] Bellenger, J., Bellenger, S., Bataille, A., Massey, K.A., Nicolaou, A. and Rialland, M. (2011) High pancreatic n-3 fatty acids prevent STZ-induced diabetes in fat-1 mice: inflammatory pathway inhibition. Diabetes 60, 1090–1099.
[10] Wirtz, S., Neufert, C., Weigmann, B. and Neurath, M.F. (2007) Chemically induced mouse models of intestinal inflammation. Nat. Protoc. 2, 541–546.
[11] Vereecke, L., Sze, M., Mc Guire, C., Rogiers, B., Chu, Y. and Schmidt-Supprian, M. (2010) Enterocyte-specific A20 deficiency sensitizes to tumor necrosis factor-induced toxicity and experimental colitis. J. Exp. Med. 207, 513–523.
[12] Zhang, J., Stirling, B., Temmerman, S.T., Ma, C.A., Fuss, I.J. and Derry, J.M. (2006) Impaired regulation of NF-κB and increased susceptibility to colitis-associated tumorigenesis in CYLD-deficient mice. J. Clin. Invest. 116, 3042–3049.
[13] Flodström, M., Tyrberg, B., Eizirik, D.L. and Sandler, S. (1999) Reduced sensitivity of inducible nitric oxide synthase-deficient mice to multiple low-dose streptozotocin-induced diabetes. Diabetes 48, 706–713.
[14] O'Brien, B.A., Harmon, B.V., Cameron, D.P. and Allan, D.J. (1996) β-Cell apoptosis is responsible for the development of IDDM in the multiple low-dose streptozotocin model. J. Pathol. 178, 176–181.
[15] Mathis, D., Vence, L. and Benoist, C. (2001) β-Cell death during progression to diabetes. Nature 414, 792–798.
[16] Kurrer, M.O., Pakala, S.V., Hanson, H.L. and Katz, J.D. (1997) β-Cell apoptosis in T cell-mediated autoimmune diabetes. Proc. Natl. Acad. Sci. USA 94, 213–218.
[17] Mauricio, D. and Mandrup-Poulsen, T. (1998) Apoptosis and the pathogenesis of IDDM: a question of life and death. Diabetes. 47, 1537–1543.
[18] Okayasu, I., Hatakeyama, S., Yamada, M., Ohkusa, T., Inagaki, Y. and Nakaya, R. (1990) A novel method in the induction of reliable experimental acute and chronic ulcerative colitis in mice. Gastroenterology 98, 694–702.
[19] Baranzini, S.E. (2009) The genetics of autoimmune diseases: a networked perspective. Curr. Opin. Immunol. 21, 596–605.
[20] Mackay, F. and Kalled, S.L. (2003) TNF ligands and receptors in autoimmunity: an update. Curr. Opin. Immunol. 14, 783–790.
[21] Wang, J. and Lenardo, M.J. (1997) Molecules involved in cell death and peripheral tolerance. Curr. Opin. Immunol. 9, 818–825.
[22] Sneller, M.C., Wang, J., Dale, J.K., Strober, W., Middelton, L.A. and Choi, Y. (1997) Clincal, immunologic, and genetic features of an autoimmune lymphoproliferative syndrome associated with abnormal lymphocyte apoptosis. Blood 89, 1341–1348.
[23] Akiyama, T., Maeda, S., Yamane, S., Ogino, K., Kasai, M. and Kajiura, F. (2005) Dependence of self-tolerance on TRAF6-directed development of thymic stroma. Science 308, 248–251.
[24] Adachi, M., Suematsu, S., Suda, T., Watanabe, D., Fukuyama, H. and Ogasawara, J. (1996) Enhanced and accelerated lymphoproliferation in Fas-null mice. Proc. Natl. Acad. Sci. USA 93, 2131–2136.
[25] Cai, X., Srivastava, S., Sun, Y., Li, Z., Wu, H. and Zuvela-Jelaska, L. (2011) Tripartite motif containing protein 27 negatively regulates CD4 T cells by ubiquitinating and inhibiting the class II PI3K-C2β. Proc. Natl. Acad. Sci. USA 108, 20072–20077.
[26] Günther, C., Martini, E., Wittkopf, N., Amann, K., Weigmann, B. and Neumann, H. (2011) Caspase-8 regulates TNF-α-induced epithelial necroptosis and terminal ileitis. Nature 477, 335–339.
[27] Nenci, A., Becker, C., Wullaert, A., Gareus, R., van Loo, G. and Danese, S. (2007) Epithelial NEMO links innate immunity to chronic intestinal inflammation. Nature 446, 557–561.